

## Spin-resolved unoccupied density of states in epitaxial Heusler-alloy films

M. Kallmayer, P. Klaer, H. Schneider, E. Arbelo Jorge, C. Herbort, G. Jakob, M. Jourdan, and H. J. Elmers\*

*Institut für Physik, Johannes Gutenberg-Universität, D-55099 Mainz, Germany*

(Received 3 April 2009; revised manuscript received 6 July 2009; published 27 July 2009)

We investigate the electronic properties of epitaxial  $\text{Co}_2(\text{Fe}_x\text{Mn}_{1-x})\text{Si}$ ,  $\text{Co}_2\text{Fe}(\text{Al}_{1-x}\text{Si}_x)$ , and  $\text{Co}_2(\text{Cr}_{0.6}\text{Fe}_{0.4})\text{Al}$  films on  $\text{MgO}(100)$  substrates using circular dichroism in x-ray absorption spectroscopy (XMCD). Considering final-state electron correlations, the spin-resolved partial density of states at the Co atom can be extracted from XMCD data. The experimental results corroborate the predicted half-metallic ferromagnetic properties of these alloys and reveal a compositional dependence of the Fermi energy position within the minority band gap.

DOI: [10.1103/PhysRevB.80.020406](https://doi.org/10.1103/PhysRevB.80.020406)

PACS number(s): 75.47.-m, 75.50.Cc, 78.70.Dm, 71.20.-b

Within the field of spintronics half-metallic ferromagnetism (HMF) plays a major role.<sup>1,2</sup> HMF stands for a metallic character of, e.g., the majority-spin states while the minority-spin states comprise an energy gap at the Fermi level.<sup>1</sup> Thus the electrical current is carried exclusively by majority-spin states making HMF materials very attractive for the fabrication of spintronic devices.<sup>3-6</sup> Co-based Heusler alloys  $\text{Co}_2YZ$  (transition-metal  $Y$  and main group element  $Z$ ) have attracted much attention in this field because *ab initio* theory has predicted HMF and a high Curie temperature for many of these compounds.<sup>1,7-9</sup> A lot of theoretical work has been devoted to the understanding of the origin of the minority band gap in Heusler compounds.<sup>7,10,11</sup> The band gap in the minority-spin states arises from the hybridization of Co and  $Y$   $3d$  orbitals. The width of the gap is determined by the Co-Co interaction because these states are closest to the Fermi energy. In order to overcome the thermally induced suppression of high spin polarization further band-structure tailoring through doping of the Heusler alloys has been proposed.<sup>6,9,12</sup> An especially interesting example is  $\text{Co}_2\text{Fe}(\text{Al}_{1-x}\text{Si}_x)$  (Ref. 6) for which *ab initio* calculations predict a Fermi energy  $E_F$  in the center of the minority gap for  $x=0.5$  in contrast to  $x=0$  and  $x=1$  with  $E_F$  positioned close to the upper or lower boundary of the gap.<sup>13,14</sup> Therefore, a direct study of the band gap is of particular importance. Although spin-resolved photoemission<sup>15,16</sup> or scanning tunneling spectroscopy can directly probe the spin polarization at a half-metal surface, these methods have no access to the crucial buried interfaces in spintronic devices.

X-ray magnetic circular dichroism (XMCD) in photoabsorption spectroscopy (XAS) is a powerful tool for studying the element-specific electronic structure at buried interfaces.<sup>17</sup> In principle, the  $L$ -edge absorption spectra for left and right circularly polarized x-ray lights reflects the spin-resolved partial density of states (PDOS) at the  $3d$  transition-metal atoms.<sup>18,19</sup> For strongly localized states, e.g., in an oxide, the strong interaction between the core hole and the conduction band in the final state leads to an additional splitting of the spectra, often denoted as multiplet effects.<sup>20</sup> These multiplet effects may effectively mask the band structure, and in this case it is impossible to disentangle the PDOS and multiplet contributions. Telling *et al.*<sup>21</sup> pointed out that the existence of local moments at the  $Y$  site in Heusler compounds also gives rise to a pronounced multiplet structure in the absorption spectra. However, previous inves-

tigations at the Co and Ni  $L$  edge in intermetallic compounds clearly revealed PDOS related features in the absorption spectra of Heusler alloys.<sup>22,23</sup>

We show that for Co-based Heusler compounds a proper consideration of the final-state effects partly recovers the spin-resolved PDOS for unoccupied Co states from the XMCD spectra. This procedure enables a direct quantitative comparison of *ab initio* calculations with experimental results. We investigate the existence of electron-electron correlation within the  $3d$  bands of the Heusler compound  $\text{Co}_2\text{FeSi}$  (Ref. 24) and the shift of the Fermi energy with respect to the minority band gap in the half-metallic compounds  $\text{Co}_2(\text{Cr}_{1-x}\text{Fe}_x)\text{Al}$ ,  $\text{Co}_2\text{Fe}(\text{Al}_{1-x}\text{Si}_x)$ , and  $\text{Co}_2(\text{Fe}_x\text{Mn}_{1-x})\text{Si}$ . We also reveal the impact of disorder on the minority band gap in  $\text{Co}_2\text{Fe}(\text{Al}_{0.3}\text{Si}_{0.7})$ .

Epitaxial  $\text{Co}_2\text{FeAl}$ ,  $\text{Co}_2\text{Fe}(\text{Al}_{0.3}\text{Si}_{0.7})$ , and  $\text{Co}_2(\text{Cr}_{0.6}\text{Fe}_{0.4})\text{Al}$  films were deposited on  $\text{MgO}(100)$  substrates employing a  $\text{MgO}$  buffer layer using rf sputtering.<sup>25</sup> Pulsed laser ablation was used to prepare epitaxial  $\text{Co}_2\text{FeSi}$ ,  $\text{Co}_2(\text{Fe}_{0.5}\text{Mn}_{0.5})\text{Si}$ , and  $\text{Co}_2\text{MnSi}$  films on  $\text{Cr}/\text{MgO}(100)$ .<sup>26</sup> The thickness was 60–100 nm and the samples were capped by 4 nm of Al in order to prevent oxidation. The characterization of the films involved x-ray diffraction (XRD), reflection of high energy electrons (RHEED), scanning tunneling microscopy (STM), and vibrating sample magnetometry (VSM). Films with  $Z=\text{Si}$  show at least partly a  $L2_1$  order, while films with  $Z=\text{Al}$  revealed a  $B2$  order, i.e., a random occupation of  $Y$  and  $Z$  sites. Details of the film properties are reported in Refs. 25 and 26.

XAS/XMCD measurements were carried out at BESSY II (beam line UE56/1-SGM). Results as shown in Fig. 1(a) were derived from total electron yield data (300 K) providing an information depth of 2.5 nm. A magnetic field of 1.6 T was applied normal to the film surface and parallel to the incident photon beam (see details in Ref. 27). The energy resolution of the x-ray monochromator was adjusted to 0.4 eV. The polarization ( $0.95 \pm 0.05$ ) was assumed to be 1 in the following.

The simplest model of resonant x-ray absorption describes the photon absorption as an excitation of a core electron into an unoccupied state.<sup>17</sup> In the proper description the atom is excited from a ground-state configuration to a final-state configuration, e.g.,  $2p^63d^7$  to  $2p^53d^8$  [see Fig. 1(b)]. In general the two models are not equivalent when open shells with more than one state need to be considered. In this case

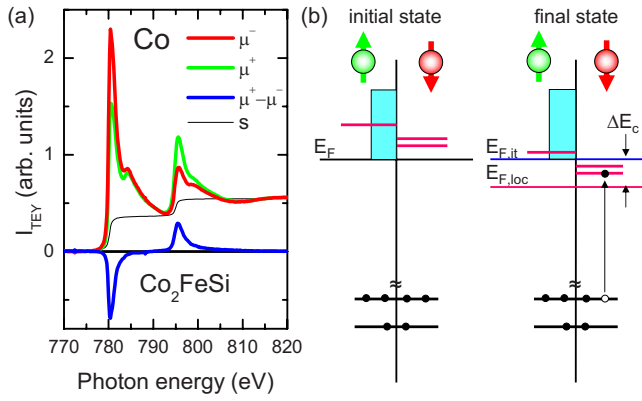


FIG. 1. (Color online) (a) XAS/XMCD data measured at the Co  $L_{3,2}$  edges of  $\text{Co}_2\text{FeSi}$ . (b) Schematic description of the absorption process emphasizing the different reference energies for the localized and the delocalized  $3d$  final-state configurations.

correlation effects between the electrons lead to multiplet effects. One may keep the one-electron model in cases where itinerant states sufficiently suppress this multiplet splitting of transition energies as, e.g., in intermetallic alloys and compounds.<sup>20</sup>

The x-ray absorption of circularly polarized light may then be explained by a two-step process considering the dipole matrix elements. In the first step, the electron is excited from a spin-orbit split  $2p_{3/2}$  or  $2p_{1/2}$  level ( $L_{3,2}$  edge) and has absorbed the angular momentum of the photon in part to its spin due to spin-orbit coupling.<sup>17</sup> Since the  $L_3$  and  $L_2$  edges have opposite spin-orbit coupling, the spin polarization is opposite at both edges. In a second step the unoccupied valence-band states serve as a detector for the spin and orbital polarization. As the orbital magnetic moment is less than 6% of the spin moment for the present samples, the orbital polarization of the photoelectrons is neglected in the following. For  $2p$  to  $3d$  transitions, the spin polarization is 25% at the  $L_3$  edge and  $-50\%$  at the  $L_2$  edge.<sup>28</sup>

Transitions from  $2p$  to  $4s$  states are largely suppressed due to the small transition matrix element. Effects from anisotropic charge and spin densities may be neglected for high crystal symmetry. Since the radial matrix elements show in general only a small energy dependence, the absorption spectra may be interpreted as a direct image of the spin-resolved PDOS above the Fermi energy.<sup>29</sup> This simple interpretation of course requires that the angular matrix elements can be averaged at every energy value; i.e.,  $3d$  states of different magnetic quantum number equally contribute to the spectral density independent of energy. We show below that these assumptions hold in the case of Co  $L$ -edge spectra of Heusler alloys.

Within the constraints discussed above, the spin-resolved unoccupied PDOS  $D^{\uparrow(\downarrow)}(1-f_F)$  (Fermi function  $f_F$ ) follows from the XAS spectra  $\mu^+$  and  $\mu^-$  according to

$$D^{\uparrow(\downarrow)}(1-f_F) \propto \mu_{iso} - s + (-) \frac{1}{P_j} \frac{\mu^+ - \mu^-}{2}, \quad (1)$$

where  $\mu_{iso}$  denotes the isotropic absorption coefficient  $(\mu^+ + \mu^-)/2$ ,  $s$  is the step function, and  $P_j$  is the spin polarization

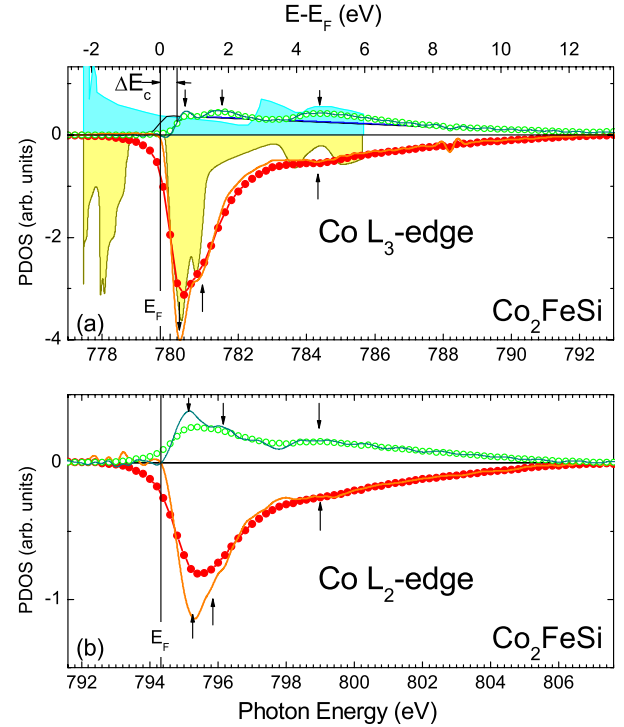


FIG. 2. (Color online) (a) Spin-resolved PDOS calculated from the XAS/XMCD data at the  $L_3$  edge. Majority PDOS (green circles) and minority PDOS (red bullets) are shown on a positive scale and negative scale, respectively. Full lines indicate deconvoluted data using a Lorentzian function (0.4 eV width). Theoretical data from Ref. 24 are shown as shaded areas. Thin black and gray (blue) lines denote the majority PDOS stemming from the itinerant band with and without consideration of the core-hole effect. (b) Spin-resolved PDOS derived from the  $L_2$ -edge data and deconvolution with 0.8 eV width. Arrows mark prominent PDOS features.

of the excited photoelectrons; i.e.,  $P_{L_3}=0.25$  and  $P_{L_2}=-0.5$ .

The result as calculated independently from both  $L$  edges is shown in Fig. 2 and compared to theoretical data.  $D^{\uparrow(\downarrow)}$  derived from the  $L_2$  edges shows a broadening compared to  $D^{\uparrow(\downarrow)}$  calculated from the  $L_3$  edges (Coster-Kronig decay).<sup>20</sup> Besides this difference in resolution the spin-resolved DOS appears similar, thus excluding an interpretation of the observed features as multiplet effects. Multiplet effects typically lead to pronounced differences between  $L_3$  and  $L_2$  edge spectra.

The minority states clearly reproduce the *ab initio* calculation. The large maximum at  $E-E_F=0.9$  eV is followed by a weak shoulder at  $E-E_F=2.5$  eV and a second peak at  $E-E_F=5$  eV. This second peak is due to a Co-Si hybridization state and shows up in the majority states, too. The onset of the majority states appears 0.5 eV above  $E_F$  instead of directly at  $E_F$ . This is a consequence of the fact that an itinerant  $3d-t_2$  band dominates the unoccupied majority states near  $E_F$  in  $\text{Co}_2\text{FeSi}$ .<sup>9</sup> The core hole in the final state attracts the electron in the localized  $3d$  states, thus lowering the photon energy needed for the transition. For an itinerant state the energy decrease is smaller since the electrons from neighboring atoms screen the core hole to some extent.<sup>30,31</sup> For a free-electron state this final-state effect would vanish and the

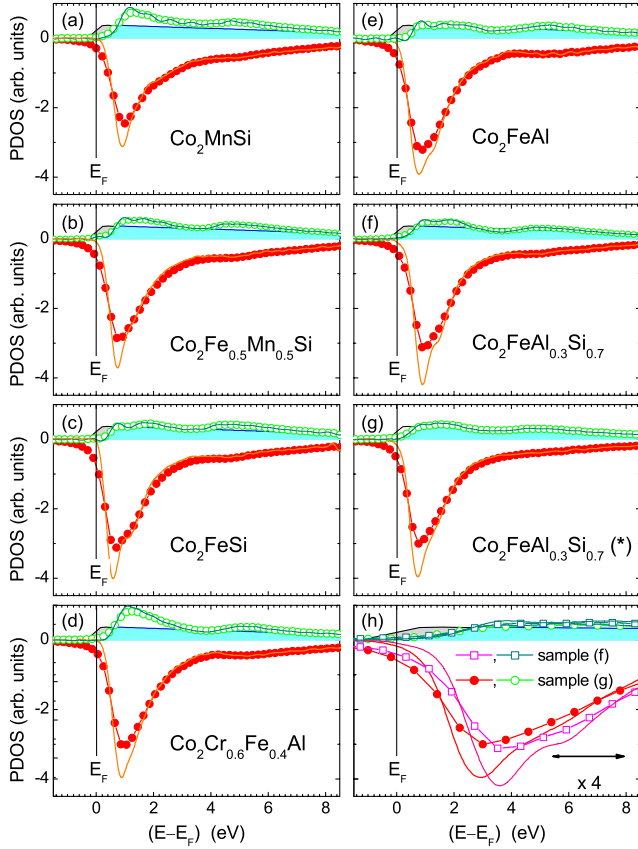


FIG. 3. (Color online) Spin-resolved PDOS calculated from the XAS/XMCD data measured at the  $L_3$  edge for samples as indicated in the figure with data representation equal to Fig. 2(a). Shadings denote the approximation of the itinerant band. (h) Comparison of the data shown in (f) and (g) on a magnified energy scale.

excitations energy equals the value following from the one-electron model. The different core-hole screening thus produces an energy shift  $\Delta E_c$  between itinerant and localized states<sup>30,31</sup> as indicated in Fig. 1(b) and accounted for by the approximated majority-spin density with and without consideration of the core hole in Fig. 2(a).

The onset of the majority PDOS indicates the Fermi edge because the minority PDOS has a band gap at  $E_F$ . In order to correct the energy scale for the localized  $3d$  states we determine  $\Delta E_c$  from comparison with calculated data for  $\text{Co}_2\text{FeSi}$  resulting in  $\Delta E_c = 0.5$  eV. In the following we assume the same value for all samples. We suggest a constant  $\Delta E_c$  for the Co-based Heusler alloys because in this case the degree of localization of the Co  $3d$  bands is similar while only their binding energies vary. This point certainly deserves further investigations because of its impact on the conclusion on half-metallic properties.

For the  $\text{Co}_2(\text{Fe}_x\text{Mn}_{1-x})\text{Si}$  film series the spin-resolved Co PDOS [Fig. 3(a)–3(c)] reveals a minority maximum at  $E_{v,\text{max}}$  approaching  $E_F$  with increasing  $x$  as depicted in Fig. 4. *Ab initio* calculations have predicted this trend, although absolute values varied depending on the model assumptions and calculation schemes.<sup>14,19,24,33–35</sup> LDA+ $U$  (Ref. 24) fits better to the experiment; however, the value of  $U$  appears overestimated for  $\text{Co}_2\text{MnSi}$ . The best agreement with experiment is

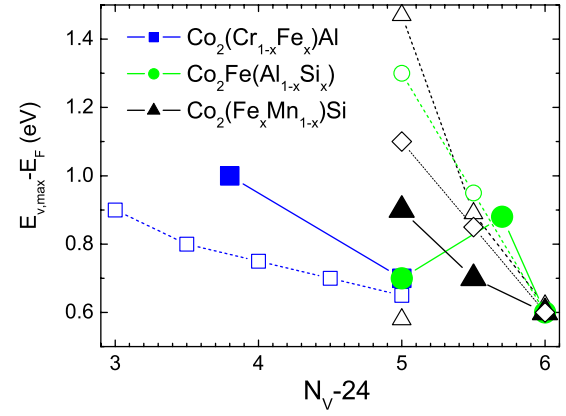


FIG. 4. (Color online) Separation of the minority PDOS maximum and the Fermi energy  $E_{v,\text{max}} - E_F$  for the indicated Heusler alloys (full symbols) compared with calculations (open symbols) using local-density approximation (LDA) [squares (Ref. 32); triangle (Ref. 33)], LDA+ $U$  [triangles (Ref. 34); circles (Ref. 14)], and LDA+DMFT [diamonds (Ref. 35)].  $N_V$  indicates the number of valence electrons per formula unit.

achieved for a recent LDA+DMFT calculation.<sup>35</sup> The rapid decrease in the minority PDOS close to  $E_F$  corroborates the predicted HMF properties. A minority Co-Fe hybridization state evolves with increasing Fe content and leads to the additional shoulder at  $E - E_F = 1$  eV. The majority PDOS decreases as expected with increasing Fe content reflecting the increasing Co magnetic moment. The PDOS of  $\text{Co}_2(\text{Fe}_{0.5}\text{Mn}_{0.5})\text{Si}$  could not be reproduced by a weighted average of  $\text{Co}_2\text{MnSi}$  and  $\text{Co}_2\text{FeSi}$  data. This excludes a phase separation and confirms the idea of band-structure tailoring.

$\text{Co}_2(\text{Cr}_{0.6}\text{Fe}_{0.4})\text{Al}$  shows the largest separation  $\Delta E_{\text{max}} = E_{v,\text{max}} - E_F$  and a steep decrease in the Co PDOS near  $E_F$ . In contrast  $\Delta E_{\text{max}}$  is strongly reduced for  $\text{Co}_2\text{FeAl}$  and the decrease near  $E_F$  is less steep. *Ab initio* calculations also reveal a trend of increasing separation with decreasing  $x$  in  $\text{Co}_2(\text{Cr}_{1-x}\text{Fe}_x)\text{Al}$ .<sup>32</sup> Accordingly, recently observed large TMR effects suggest a high spin polarization for  $\text{Co}_2(\text{Cr}_{0.6}\text{Fe}_{0.4})\text{Al}$ .<sup>36</sup>

The Co PDOS of  $\text{Co}_2\text{Fe}(\text{Al}_{0.3}\text{Si}_{0.7})$  is quite similar to that of  $\text{Co}_2\text{FeSi}$ , with increased  $\Delta E_{\text{max}}$ . This trend was predicted by a LDA+ $U$  calculation.<sup>14</sup> However, the same calculation showed an even larger value for  $\text{Co}_2\text{FeAl}$  which is in disagreement with our experimental result but may be explained by the B2 order in the latter films.

We also investigated a second  $\text{Co}_2\text{Fe}(\text{Al}_{0.3}\text{Si}_{0.7})$  film [Fig. 3(g)] that has been prepared with lower annealing temperature (450 C instead of 550 C) revealing a B2 structure instead of the  $L2_1$  structure observed for the sample in Fig. 3(f). In this case  $\Delta E_{\text{max}}$  is reduced and the minority PDOS peak is broader compared to the  $L2_1$  film.

In summary, we present a calculation scheme for recovering the spin-resolved unoccupied Co PDOS in Co-based Heusler alloys from XMCD. The scheme has been applied to epitaxial  $\text{Co}_2(\text{Fe}_x\text{Mn}_{1-x})\text{Si}$  and  $\text{Co}_2\text{Fe}(\text{Al}_{1-x}\text{Si}_x)$  films grown on MgO(100). We observed a variation in the position of  $E_F$

within the minority band gap with the substitution of the transition-metal element or the main group element in agreement with earlier predictions. We note that  $\Delta E_c$  may strongly vary the measured minority PDOS at  $E_F$ . Consequently, half-metallicity cannot unambiguously be proven with this method. The comparison with theory, however, allows an estimation of theoretical parameters, e.g., the electron-electron correlation potential. For  $\text{Co}_2\text{Fe}(\text{Al}_{0.3}\text{Si}_{0.7})$  we ob-

served a broadening of the minority PDOS with increased local disorder. These examples suggest that XMCD provides a pathway for the improvement of HMF materials and interfaces for spintronic devices.

The authors are thankful for financial support from the DFG (Grant No. FOR 559) and BMBF (Grant No. ES3XBA/5) and S. Cramm for support at BESSY.

\*elmers@uni-mainz.de

- <sup>1</sup>R. A. de Groot, F. M. Mueller, P. G. van Engen, and K. H. J. Buschow, *Phys. Rev. Lett.* **50**, 2024 (1983).
- <sup>2</sup>J. H. Park, E. Vescovo, H. J. Kim, C. Kwon, R. Ramesh, and T. Venkatesan, *Nature (London)* **392**, 794 (1998).
- <sup>3</sup>K. Inomata, S. Okamura, R. Goto, and N. Tezuka, *Jpn. J. Appl. Phys.* **42**, L419 (2003).
- <sup>4</sup>S. Kammerer, A. Thomas, A. Hütten, and G. Reiss, *Appl. Phys. Lett.* **85**, 79 (2004).
- <sup>5</sup>Y. Sakuraba, M. Hattori, M. Oogane, Y. Ando, H. Kato, A. Sakuma, T. Miyazaki, and H. Kubota, *Appl. Phys. Lett.* **88**, 192508 (2006).
- <sup>6</sup>W. Wang, H. Sukegawa, R. Shan, and K. Inomata, *Appl. Phys. Lett.* **93**, 122506 (2008).
- <sup>7</sup>I. Galanakis, P. H. Dederichs, and N. Papanikolaou, *Phys. Rev. B* **66**, 174429 (2002).
- <sup>8</sup>S. Picozzi, A. Continenza, and A. J. Freeman, *Phys. Rev. B* **66**, 094421 (2002).
- <sup>9</sup>C. Felser, G. Fecher, and B. Balke, *Angew. Chem., Int. Ed.* **46**, 668 (2007).
- <sup>10</sup>I. Galanakis, Ph. Mavropoulos, and P. H. Dederichs, *J. Phys. D* **39**, 765 (2006).
- <sup>11</sup>H. C. Kandpal, G. H. Fecher, and C. Felser, *J. Phys. D* **40**, 1507 (2007).
- <sup>12</sup>L. Chioncel, Y. Sakuraba, E. Arrigoni, M. I. Katsnelson, M. Oogane, Y. Ando, T. Miyazaki, E. Burzo, and A. I. Lichtenstein, *Phys. Rev. Lett.* **100**, 086402 (2008).
- <sup>13</sup>Z. Gercsi and K. Hono, *J. Phys.: Condens. Matter* **19**, 326216 (2007).
- <sup>14</sup>G. H. Fecher and C. Felser, *J. Phys. D* **40**, 1582 (2007).
- <sup>15</sup>W. H. Wang, M. Przybylski, W. Kuch, L. I. Chelaru, J. Wang, Y. F. Lu, J. Barthel, H. L. Meyerheim, and J. Kirschner, *Phys. Rev. B* **71**, 144416 (2005).
- <sup>16</sup>H. Schneider, G. Jakob, M. Kallmayer, H. J. Elmers, M. Cinchetti, B. Balke, S. Wurmehl, C. Felser, M. Aeschlimann, and H. Adrian, *Phys. Rev. B* **74**, 174426 (2006).
- <sup>17</sup>J. Stöhr, *J. Magn. Magn. Mater.* **200**, 470 (1999).
- <sup>18</sup>H. Ebert, *Rep. Prog. Phys.* **59**, 1665 (1996).
- <sup>19</sup>V. N. Antonov, D. A. Kukusta, A. P. Shpak, and A. N. Yaresko, *Condens. Matter Phys.* **11**, 627 (2008).
- <sup>20</sup>F. M. F. de Groot, J. C. Fuggle, B. T. Thole, and G. A. Sawatzky, *Phys. Rev. B* **42**, 5459 (1990).
- <sup>21</sup>N. D. Telling, P. S. Keatley, G. van der Laan, R. J. Hicken, E. Arenholz, Y. Sakuraba, M. Oogane, Y. Ando, K. Takanashi, A. Sakuma, and T. Miyazaki, *Phys. Rev. B* **78**, 184438 (2008).
- <sup>22</sup>M. Kallmayer, K. Hild, T. Eichhorn, H. Schneider, G. Jakob, A. Conca, M. Jourdan, H. J. Elmers, A. Gloskovskii, S. Schuppler, and P. Nagel, *Appl. Phys. Lett.* **91**, 192501 (2007).
- <sup>23</sup>G. Jakob, T. Eichhorn, M. Kallmayer, and H. J. Elmers, *Phys. Rev. B* **76**, 174407 (2007).
- <sup>24</sup>H. C. Kandpal, G. H. Fecher, C. Felser, and G. Schönhense, *Phys. Rev. B* **73**, 094422 (2006).
- <sup>25</sup>C. Herbort, E. Arbelo Jorge, and M. Jourdan, *J. Phys. D* **42**, 084006 (2009).
- <sup>26</sup>H. Schneider, E. Vilanova, B. Balke, C. Felser, and G. Jakob, *J. Phys. D* **42**, 084012 (2009).
- <sup>27</sup>M. Kallmayer, H. Schneider, G. Jakob, H. J. Elmers, K. Kroth, H. Kandpal, U. Stumm, and C. Cramm, *Appl. Phys. Lett.* **88**, 072506 (2006).
- <sup>28</sup>J. Stöhr, *J. Electron Spectrosc. Relat. Phenom.* **75**, 253 (1995).
- <sup>29</sup>J. Kunes and P. M. Oppeneer, *Phys. Rev. B* **67**, 024431 (2003).
- <sup>30</sup>P. J. W. Weijs, M. T. Czyzyk, J. F. van Acker, W. Speier, J. B. Goedkoop, H. van Leuken, H. J. M. Hendrix, R. A. de Groot, G. van der Laan, K. H. J. Buschow, G. Wiech, and J. C. Fuggle, *Phys. Rev. B* **41**, 11899 (1990).
- <sup>31</sup>A. Bianconi, *Phys. Rev. B* **26**, 2741 (1982).
- <sup>32</sup>G. H. Fecher, H. C. Kandpal, S. Wurmehl, J. Morais, H. Lin, H. J. Elmers, G. Schönhense, and C. Felser, *J. Phys.: Condens. Matter* **17**, 7237 (2005).
- <sup>33</sup>K. Özdoğan, B. Aktas, I. Galanakis, and E. Sasioglu, *J. Appl. Phys.* **101**, 073910 (2007).
- <sup>34</sup>B. Balke, G. H. Fecher, H. C. Kandpal, C. Felser, K. Kobayashi, E. Ikenaga, J.-J. Kim, and S. Ueda, *Phys. Rev. B* **74**, 104405 (2006).
- <sup>35</sup>S. Chadov, G. H. Fecher, C. Felser, J. Minar, J. Braun, and H. Ebert, *J. Phys. D* **42**, 084002 (2009).
- <sup>36</sup>C. Herbort, E. Arbelo Jorge, and M. Jourdan, *Appl. Phys. Lett.* **94**, 142504 (2009).